

Size-independent residual magnetic moments of colloidal Fe₃O₄-polystyrene nanospheres detected by ac susceptibility measurements

Du-Xing Chen,^{1,a)} Alvaro Sanchez,² Hong Xu,³ Hongchen Gu,³ and Donglu Shi^{3,4}

¹ICREA and Departament de Física, Universitat Autònoma de Barcelona, 08193 Bellaterra, Spain

²Departament de Física, Universitat Autònoma de Barcelona, 08193 Bellaterra, Spain

³Research Institute for Micro/Nano Science and Technology, Shanghai Jiaotong University, Shanghai 200030, China

⁴Department of Chemical and Materials Engineering, University of Cincinnati, Cincinnati, Ohio 45221, USA

(Received 16 May 2008; accepted 9 September 2008; published online 3 November 2008)

Complex ac susceptibility of magnetic colloids of nanospheres, each consisting of Fe₃O₄ nanoparticles densely and uniformly embedded in a polystyrene matrix, is measured as a function of frequency. A data analysis based on a model and the directly measured size distribution shows that each spherical aggregate of nanoparticles carries a small residual magnetic moment, whose average is basically independent of the sphere size. The mentioned model assumes that magnetic spheres undergo rotational Brownian motions obeying Debye's theory and nanoparticles undergo Néel magnetization rotations. A discussion is made on the superparamagnetism and the nanoparticle interactions in the present case, in order to justify the applicability of the model and to look for the mechanism of the detected sphere-size independent magnetic moment. © 2008 American Institute of Physics. [DOI: 10.1063/1.3005988]

I. INTRODUCTION

A process was developed to produce colloids of nanoscaled magnetite/polystyrene (Fe₃O₄/PS) spheres with a dense and uniform magnetic occupation and a narrow size distribution, for satisfying the requirements of biomedical applications.¹ The dense magnetic occupation was detected by high-field magnetic measurements. It should be of interest also to study their low-field properties, since magnetic colloids are often used at low fields. Connolly and St Pierre² proposed an ac susceptibility technique to detect the hydrodynamic sizes of magnetic colloids. They also proposed a method to consider the size distribution, of which further analysis was carried out by Nutting *et al.*³ In the present work, we measure frequency dependent complex ac susceptibility $\chi = \chi' - j\chi''$ of two samples prepared with the above mentioned process and use the technique proposed in Ref. 2 to analyze the results. We will show that in spite of a high saturation magnetization and a certain size distribution of the nanospheres, each sphere carries only a tiny residual magnetic moment and the average moment is roughly independent of the sphere size. This phenomenon is intimately related to the nanostructure of the samples, which is explained in Sec. II, and studied by a model fit to the experimental data in Sec. III. For understanding the physics behind it, the superparamagnetism and particle interactions in the present case are deeply discussed in Sec. IV. The conclusions are presented in Sec. V.

II. SAMPLES AND MEASUREMENTS

Colloids A and B were prepared as described in Ref. 1 but without a silica coating. Many Fe₃O₄ (verified by x-ray

diffraction measurements) nanoparticles of diameter 10 nm [as observed by transmission electron microscopy (TEM)] were uniformly embedded in a nanoscaled spherical PS matrix, and many such Fe₃O₄/PS nanospheres were suspended in a 0.5 wt % Tween 20 solution. The polysorbate surfactant Tween 20 was used as a wetting agent to stabilize the suspension; without it, nanospheres would sink quickly to the bottom.⁴ The suspension concentration was measured to be 1.12 and 0.90 wt % for colloids A and B, respectively. The averaged magnetite content in the dried state was determined by thermogravimetric analysis (TGA2050, TA Instruments) to be 69 and 71 wt % for colloids A and B, respectively. The remaining 31 and 29 wt % came from the PS and the surface modification agent. The hydrodynamic size distribution of the nanospheres, p_i versus D_i , was determined using a high-performance particle sizer (model HPP5001, Malvern Siber Hegner) based on the detection of translational Brownian motion by dynamic light scattering. The results are plotted in Fig. 1.

The dependence of the complex ac susceptibility χ on frequency $f = \omega/2\pi$ was measured at 296 K with an ac susceptometer using Helmholtz coils as magnetizer.⁵ The susceptometer was calibrated using a copper disk as the standard sample.⁶ For the measurements, glass bottles containing about 0.8 cm³ of colloid A or B served as sample A or B. The field amplitude was set below 100 A/m to ensure the measured χ be the low-field limit required by a relevant model of Brownian rotations (see Sec. IV). The results are plotted in Figs. 2(a) and 2(b) for samples A and B, respectively. For both samples, with increasing f from 10 to 20 000 Hz, χ' decreases from a stable high value to a stable low value, which is accompanied by a $\chi''(f)$ peak.

^{a)}Electronic mail: duxing.chen@uab.es.

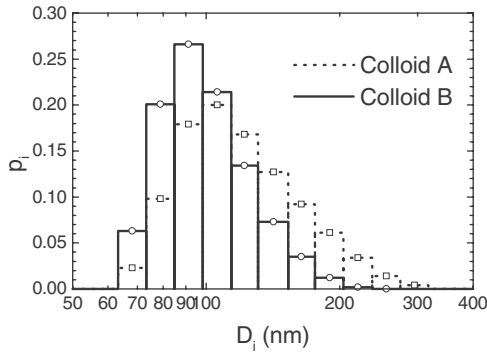


FIG. 1. The number distribution of nanospheres for colloids A and B as a function of hydrodynamic size. The i th column corresponds to the sphere number fraction p_i for a diameter interval, in logarithmic scale, centered at D_i marked by a symbol.

III. ANALYSIS OF EXPERIMENTAL RESULTS

A. Model

In the literature,⁷⁻¹¹ the above feature has been interpreted as arising from two contributions. The first originates from the ac field driven rotational Brownian motions of magnetic spheres and the other from the ac field driven Néel magnetization rotations within the nanoparticles:

$$\chi(\omega) = \chi_B(\omega) + \chi_N(\omega) = \chi'_B(\omega) + \chi_{N0} - j\chi''_B(\omega), \quad (1)$$

where we have assumed that the Néel susceptibility $\chi_N(\omega)$ equals its low- ω limit χ_{N0} with $\chi''_N(\omega)=0$. A general analysis for the Brownian susceptibility $\chi_B(\omega)$ is carried out as follows.

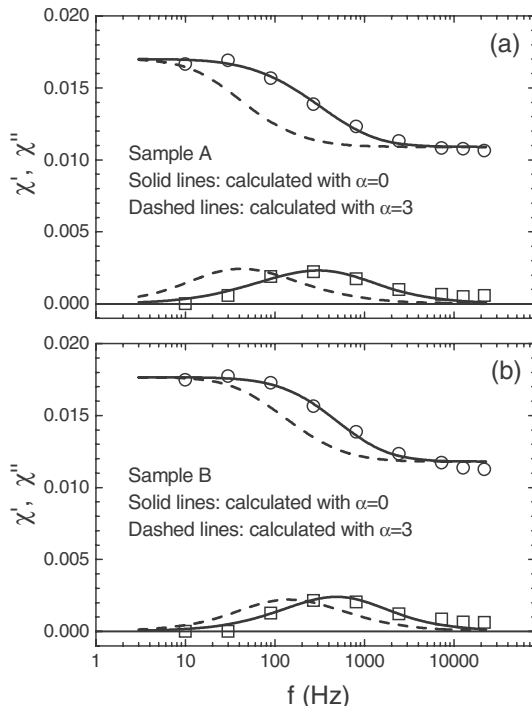


FIG. 2. The measured complex low-field ac susceptibility of samples A and B as a function of frequency (symbols) compared with modeling results assuming a sphere-size independent moment (solid lines) and a moment proportional to sphere volume (dashed lines).

Parallel to Debye's theory for the electric susceptibility of spherical polar molecules undergoing rotational Brownian motion in a liquid,¹² the complex low-field magnetic susceptibility $\chi_B = \chi'_B - j\chi''_B$ of magnetic spheres of number density n with identical magnetic moment m_0 and identical hydrodynamic diameter D suspended in a liquid of viscosity η at angular frequency ω is expressed by

$$\chi_B(\omega, D) = \frac{\chi_{B0}}{1 + j\omega\tau(D)} = \frac{\chi_{B0}}{1 + [\omega\tau(D)]^2} - j \frac{\chi_{B0}\omega\tau(D)}{1 + [\omega\tau(D)]^2}, \quad (2)$$

where the low ω limit of χ_B is^{12,13}

$$\chi_{B0} = \frac{n\mu_0 m_0^2}{3k_B T}, \quad (3)$$

and the Brownian relaxation time is¹²

$$\tau(D) = \frac{\pi\eta D^3}{2k_B T}. \quad (4)$$

If there is a distribution in D between D_{\min} and D_{\max} with a number probability density $p(D)$, χ_{B0} should be replaced by its average,

$$\chi_{B0,av} = \frac{n\mu_0 [m_0^2(D)]_{av}}{3k_B T}, \quad (5)$$

where $m_0(D)$ has been assumed to be the moment of the spheres with hydrodynamic diameter D , so that the averaged $m_0^2(D)$ over all sizes is calculated by

$$[m_0^2(D)]_{av} = \int_{D_{\min}}^{D_{\max}} m_0^2(D) p(D) dD. \quad (6)$$

Replacing χ_{B0} in Eq. (2) by $\chi_{B0,av}$ in Eq. (5) and averaging $\chi_B(\omega, D)$ with respect to D , we obtain the final result

$$\begin{aligned} \chi_B(\omega) &= \int_{D_{\min}}^{D_{\max}} \chi_B(\omega, D) p(D) dD \\ &= \frac{\chi_{B0,av}}{[m_0^2(D)]_{av}} \int_{D_{\min}}^{D_{\max}} \frac{m_0^2(D) p(D)}{1 + j\omega\tau(D)} dD \\ &= \frac{\chi_{B0,av}}{[m_0^2(D)]_{av}} \int_{D_{\min}}^{D_{\max}} \frac{m_0^2(D) p(D)}{1 + [\omega\tau(D)]^2} dD \\ &\quad - \frac{j\chi_{B0,av}}{[m_0^2(D)]_{av}} \int_{D_{\min}}^{D_{\max}} \frac{m_0^2(D) \omega\tau(D) p(D)}{1 + [\omega\tau(D)]^2} dD. \end{aligned} \quad (7)$$

Using this model, the measured $\chi(\omega)$ curves for both samples may be simulated by Eqs. (1) and (7).

B. Simulation to experimental results

For the simulation, we use $\eta=0.933$ mPa s for water at $T=296$ K,¹⁴ $\mu_0=4\pi \times 10^{-7}$ H/m, $k_B=1.38 \times 10^{-23}$ J/K, and the directly measured p_i versus D_i , which is a discrete version of $p(D)$, in Fig. 1. $m_0(D)$ is generally approximated by

$$m_0(D) \propto D^\alpha, \quad (8)$$

where α is a constant. Adjusting the values of fitting parameters $\chi_{B0,av}$, χ_{N0} , and α to simulate the low- f portion of the measured results, we find that only when α is near zero may both $\chi'(f)$ and $\chi''(f)$ be well fitted by Eqs. (1) and (7) with $\chi_{B0,av}=0.0061$ and $\chi_{N0}=0.0109$ for sample A and $\chi_{B0,av}=0.00585$ and $\chi_{N0}=0.0118$ for sample B. The calculated curves for $\alpha=0$ are plotted by solid lines in Fig. 2.

C. Size-independent residual magnetic moment of nanospheres

The value of $\alpha=0$ in Eq. (8) means that $m_0(D)$ is a constant, i.e., each sphere carries a moment that is independent of sphere size. In contrast, one could have expected another case as follows. When magnetic nanoparticles are uniformly distributed in the spheres, the saturation magnetization of each sphere should be the same, and it would be reasonable that each sphere also has the same residual magnetization M_r at zero field. This would correspond to $\alpha=3$. Replacing $\alpha=0$ in the above simulation by $\alpha=3$, the calculated results are plotted in Fig. 2 by dashed lines. We see that compared with the experimental data, all these lines are remarkably shifted to low frequencies, so the possibility of $\alpha=3$ is ruled out. We should mention that for magnetic colloids of nonaggregate nanoscaled cobalt ferrites, $\alpha=3$ is basically valid.¹⁵

Hence, we can state that the residual moment m_0 of every magnetic nanosphere is basically the same but not proportional to its volume, as would be derived from a constant residual magnetization M_r , in spite of the large variation in the sphere volume covering a range of two orders of magnitude. Not only is m_0 nearly constant, but m_0 is also very small in comparison with the saturation moment m_s in each sphere, as estimated below.

D. Smallness of nanosphere moment

Since two samples are similar, we give our estimates for sample A only. Assuming the density of the magnetite and the remainder solids to be 5.24 (Ref. 13) and 1.15 g/cm³, respectively, and knowing the weight percentage for the magnetite and the rest solids to be 69 and 31, respectively, the 1.12 wt % of solid spheres in the liquid may be converted to 0.45 vol %. The averaged volume per sphere is calculated as

$$v_{av} = \frac{\pi}{6} \int_{D_{min}}^{D_{max}} D^3 p(D) dD = 1.37 \times 10^6 \text{ nm}^3. \quad (9)$$

Thus, a number density $n=3.28 \times 10^{18} \text{ m}^{-3}$ is obtained from the ratio from 4.5×10^{24} to $1.37 \times 10^6 \text{ nm}^3$. Substituting $\chi_{B0,av}=0.0061$ and this n value in Eq. (5), we obtain

$$m_0 = \left(\frac{3k_B T \chi_{B0,av}}{n \mu_0} \right)^{1/2} = 4.3 \times 10^{-18} \text{ A m}^2. \quad (10)$$

Assuming $\mu_0 M_s(\text{Fe}_3\text{O}_4)$ at 296 K to be 0.60 T, estimated from the magnetization data in Ref. 1, the moment m_0 per nanoparticle of magnetite of diameter 10 nm is estimated to be $2.5 \times 10^{-19} \text{ A m}^2$. Thus, the m_0 carried by each magnetic

nanosphere corresponds to the total moment of about 17 nanoparticles when their moments are parallel. Since the smallest and largest spheres contain 10^2 and 10^4 nanoparticles, m_0 turns out to be about 20% and 0.2% of m_s for the smallest and largest spheres, respectively.

E. Comparison with previous works

We now come back to Connolly and St Pierre's proposition.² They have assumed a normal Gaussian distribution function for $p(D)$, by which the average is carried out considering the distributed $\tau(D)$ but disregarding a distribution in $m_0(D)$. In fact, such an omission could be justified by our result of $m_0(D)=m_0$. Nutting *et al.*³ have added another possible log-normal distribution to $p(D)$, which has been used by Claesson *et al.*¹¹ to analyze their ac susceptibility measurements of colloids containing monodispersed silica-cobalt ferrite microspheres. In their case, CoFe_2O_4 particles of 16.8 nm in diameter and $\mu_0 M_s=0.53 \text{ T}$ are uniformly planted on a silica sphere surface to form a magnetic microsphere,¹⁶ and the measured χ curves were well fitted without considering the $m_0(D)$ distribution. Although a particular log-normal distribution of $p(D)$ rather than a measured p_i versus D_i function was chosen for the fit in Ref. 11, it seems that our statement of a uniform m_0 is also valid for their case, where the experimental moment per microsphere $m_0=2.5 \times 10^{-17} \text{ A m}^2$ corresponds to the moment of about 24 magnetic nanoparticles when their moments are parallel. Therefore, the results of previous works on nanospheres consisting of many single-domain particles are consistent with the tiny and basically size-independent residual moment discovered in the present work, and a further analysis on this general feature is of great interest.

F. High-frequency susceptibility

It should be mentioned that there is a small error in the above m_0 estimate, since the hydrodynamic D has been used to stand for the diameter of solid sphere; the hydrodynamic sphere should be larger than the solid one by a bonded thin water layer.¹¹

Another phenomenon is necessary to be studied further: χ' and χ'' at high f are not constant and zero, respectively, as characterized by Néel magnetization rotation. This phenomenon may be attributed to the presence of nanospheres with sizes around 30 nm. We can estimate from Eq. (4) that $\tau(D)$ is on the order of 10^{-5} s when $D=30 \text{ nm}$, which will result in a χ_B with maximum χ''_B occurring at $\sim 1.6 \times 10^4 \text{ Hz}$, i.e., the frequency around which the anomaly occurs. In order to check if this idea is correct or not, we have made TEM observation of some dried colloid A and found the presence of such "nanospheres" (of irregular shapes) as shown in Fig. 3. The volume percentage of such nanospheres are extremely small, but since each of such small spheres has the same moment m_0 as the much larger ones, their contribution to χ_B becomes quite large.

On the other hand, the high-performance particle sizer measures the sizes, between 0.6 and 6000 nm, of spherical particles by analyzing the intensity fluctuations of the Rayleigh scattering laser light without assuming any special size

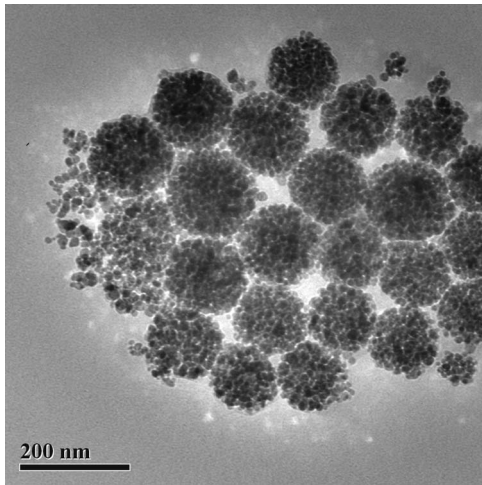


FIG. 3. A TEM picture of dried colloid A.

distribution so that the 30 nm small nanospheres should be detectable. However, repeating several times careful measurements, we did not find any spheres of $D < 63$ nm by this technique. It seems that the translational Brownian motions of such small particles are coupled to those of larger ones in the colloid, so that the scattering by small particles themselves with an extremely small volume fraction becomes negligible. If this is true and as long as there is a size-independent moment, we may state that our ac susceptibility technique is more sensitive than the high-performance particle sizer to detect the presence of very small magnetic particles in colloids.

IV. SUPERPARAMAGNETISM

A. Classical definition of superparamagnetism

The concept of superparamagnetism was first proposed by Bean,¹⁷ who referred a dilute assembly of ferromagnetic particles as superparamagnetic if the particles were single domain and when the thermal energy at the temperature of the experiment was sufficient to equilibrate the magnetization of the assembly in a time short compared with that of the experiment.

Assuming the particle number density to be n and each particle to carry a moment m_0 , the thermal equilibrium magnetization M as a function of field H is calculated by the Langevin function $L(x)$ as

$$M = M_0 L(x) = M_0 (\coth x - 1/x), \quad (11)$$

where $M_0 = nm_0$ and $x = \mu_0 m_0 H / k_B T$. We have used M_0 to stand for nm_0 rather than using the saturation magnetization M_s . This is because that M_s is exclusively used in the present paper for the saturation magnetization of ferrite materials and that nm_0 is not always a saturation magnetization when Eq. (11) is used. This second reason is conceptually essential for us to use the superparamagnetism theory for the present colloids of magnetic nanospheres, as will be discussed below.

In order to achieve the equilibrium, the time for either of the following two kinds of relaxation should be less than the time of an experiment.¹⁸ If spherical particles are suspended in a liquid medium so that the equilibrium is approached by

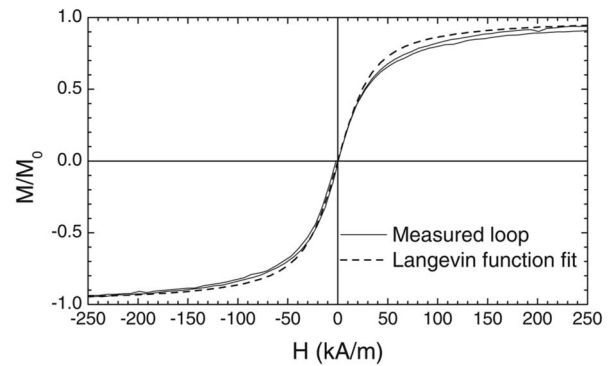


FIG. 4. For a powder sample consisting of silica coated nanospheres with densely packed 10 nm Fe_3O_4 particles, the low-field portion of the hysteresis loop (solid lines) obtained by semiconducting quantum interference device (SQUID) measurements at 300 K between $\pm 8 \times 10^5$ A/m. Dashed line is calculated from Eq. (11). The hysteresis is partially due to that of the superconducting magnet used in the SQUID magnetometer.

physical Brownian rotations of individual particles, the relaxation time is calculated by Eq. (4). If the particles are physically fixed, the equilibrium is realized by thermally activated moment rotations proposed by Néel¹⁹ with time constant τ determined by

$$\tau = \tau_0 \exp(K_{\text{eff}} v / k_B T), \quad (12)$$

where τ_0 has the order of 10^{-9} s, v is the particle volume, and K_{eff} is an effective anisotropy constant.

B. Superparamagnetism for the assembly of Fe_3O_4 nanoparticles

If we want to use the classical definition of superparamagnetism for the assembly of Fe_3O_4 nanoparticles, which are densely packed within each nanosphere, then “ferromagnetic particles” should be modified to include ferrimagnetic ones and the constraint of “dilute” should be temporarily relaxed.

We have measured at 300 K the saturated dc magnetization loop of a powder sample consisting of nanospheres being the same as the present ones but with 10 nm silica coating. A low-field portion of the results is plotted in Fig. 4 by solid lines and it is rather well fitted by the Langevin function [Eq. (11)], as the dashed line. From the fitting parameter $m_0 = 2.35 \times 10^{-19}$ A m² and $\mu_0 M_s = 0.60$ T, we obtain the particle diameter to be 9.8 nm, which is consistent with the directly observed nanoparticle size. This result indicates that although the nanoparticles are densely packed within each nanosphere, they are apparently superparamagnetic. The Néel relaxation time constant may be estimated as follows. Since the cubic anisotropy constant of Fe_3O_4 at 300 K is $K_1 = -1.1 \times 10^4$ J/m³,¹³ we have $K_{\text{eff}} = -K_1/12 \approx 1 \times 10^3$ J/m³,¹⁸ so that $\tau \approx 2 \times 10^{-5}$ s is estimated from $v = 5 \times 10^{-23}$ m³. It is much smaller than the time of dc magnetic measurement, so that the obtained magnetization is equilibrate. The small hysteresis and departure from the fitting curve may result partially from the interaction among the densely packed particles.

C. Magnetostatic interaction

The interaction between neighboring magnetic particles may be estimated by point moment approximation. The dipolar interaction energy U_{12} between two point moments \mathbf{m}_i at \mathbf{r}_i ($i=1$ and 2) with $\mathbf{r}_{12}=\mathbf{r}_1-\mathbf{r}_2$ is calculated by¹³

$$U_{12} = \frac{\mu_0}{4\pi r_{12}^3} \left[\mathbf{m}_1 \cdot \mathbf{m}_2 - \frac{3}{r_{12}^2} (\mathbf{m}_1 \cdot \mathbf{r}_{12})(\mathbf{m}_2 \cdot \mathbf{r}_{12}) \right]. \quad (13)$$

Assuming $m_1=m_2=m_0=2.5 \times 10^{-19}$ A m² for particles of diameter 10 nm so that $r_{12}=10$ nm, we obtain from Eq. (13) that $U_{12}=-1.2 \times 10^{-20}$ or 6×10^{-21} J when $\mathbf{m}_{1,2}$ are in the same direction that is along or perpendicular to \mathbf{r}_{12} , respectively, and that both values change their signs if $\mathbf{m}_{1,2}$ are opposite. Since the energy difference between different relative moment directions is larger than $k_B T \approx 4 \times 10^{-21}$ J, the particles should be distributed in a structure with a minimum magnetostatic energy roughly corresponding to the sum of relevant U_{12} values. As a result, some kind of random “antiferromagnetic” moment orientations will occur with dominant elementary interaction U_{12} to be close to -1.2×10^{-20} and -6×10^{-21} J.

This antiferromagnetic coupling is equivalent to a unidirectional anisotropy for each nanoparticle. If the easy directions of such anisotropy for all the nanoparticles are uniformly distributed in all directions, then this coupling does not change the low-field $M(H)$ of the superparamagnetism of Néel rotations, just like that the uniaxial or cubic magnetocrystalline anisotropies do not influence the low-field $M(H)$ of superparamagnetism described in Ref. 18. Thus, by fitting the low-field $M(H)$ in Fig. 4, we obtain the correct particle size. This coupling may be an origin of the hysteresis in the $M(H)$ curve. At higher $|H|$, the fact that $|M|$ is lower than the calculated one shown in Fig. 4 may also be attributed to the antiferromagnetic coupling, which impedes the parallel process. It seems that the magnetostatic U_{12} is not large enough to completely account for the hysteresis and the overlow $|M|$ at intermediate values of $|H|$, and the exchange interaction between mutually touched nanoparticles may play an important role to reinforce these features.

Thus, with magnetostatic and possible exchange interactions among densely packed single-domain particles, the assembly of Fe₃O₄ nanoparticles shows approximately a superparamagnetic $M(H)$ curve.

D. Superparamagnetism for the assembly of nanospheres

With antiferromagnetic coupling within each nanosphere, the magnetic moment per nanosphere is ideally zero if its constituting nanoparticles form a large perfect regular array. A small moment is expected to occur for any real nanosphere where the nanoparticles are located randomly with some voids and whose shape is not perfectly spherical. A size-independent moment is not deducible, but it may be expected that when an aggregation contains a few particles, most particle moments will be in the same direction to achieve the lowest U_{12} .²⁰ For the present case where the sphere sizes are not very small, it is most possible that there

is a certain moment distribution for the spheres with a given size and the averaged moment for the distribution is roughly independent of the sphere size.

To apply the above classical definition of superparamagnetism to the assembly of the nanospheres, the single-domain condition has to be removed since each nanosphere contains many single-domain Fe₃O₄ particles. Generally speaking, when each particle contains a number of domains, a dilute assembly of the particles can behave as superparamagnetic if each particle carries a fixed moment m_0 . For our case, the condition of “fixed moment” can be quite well met when $x = \mu_0 m_0 H / k_B T \ll 1$, where $m_0 = 2.35 \times 10^{-19}$ A m², holds for the Néel rotations so that the antiferromagnetism is not overcome by the applied field. Obviously, M_0 in Eq. (11) for the superparamagnetism of the assembly of nanospheres cannot be understood as the saturation magnetization M_s . This M_0 is well defined only at low fields by nm_0 and this superparamagnetism will be completely destroyed at fields much smaller than the saturation field.

There should be another modification introduced to the classical definition of superparamagnetism; the assembly is not necessarily thermally equilibrate. In fact, while the dc property of a superparamagnetic assembly is generally expressed by Eq. (11), the low-field limit of its ac property in liquid is expressed by Eq. (2). For the Brownian rotations with $m_0 = 4.3 \times 10^{-18}$ A m² for the spheres, $x=1$ corresponds to $H=770$ A/m, so that low fields mean that $H_m \ll 770$ A/m. This condition has been met in our measurements.

The occurrence of a permanent magnetic moment in small antiferromagnetic particles has been studied conceptually by Néel.²¹ He states that there is no good reason why the two antiferromagnetic sublattices should contain exactly the same number of magnetic atoms, and the particle should, in practice, exhibit a slight ferrimagnetism. The permanent magnetic moment, equal to the difference in spontaneous magnetizations of both sublattices, becomes relatively greater the smaller the particle. Adopting different hypotheses, he suggests that the net moment is proportional to a $\frac{1}{3}$ to $\frac{2}{3}$ power of the number of spins, so slowly increases with the particle size. Our case is similar to his case if the nanoparticles and nanospheres are understood as his spins and particles, respectively. However, his suggestion corresponds to $\alpha=1$ to 2 in Eq. (8), different from our discovery of $\alpha=0$ for the nanospheres.

E. Summary remarks

After the above analysis on the superparamagnetism and particle interactions, it is worthy giving some summary remarks. Both the assembly of nanoparticles and the assembly of nanospheres are partially superparamagnetic, since they satisfy some but not all necessary conditions required by the classical definition of superparamagnetism.

The nanoparticles are single domain and undergoing Néel rotations. The time constant of Néel rotations is on the order of 10 μ s, which is much smaller than our dc and ac measurement time, so that the dc and ac $M(H)$ of the assembly follows basically Eq. (11). The assembly of nanoparticles

is partially superparamagnetic since it is not dilute and there is a certain antiferromagnetic interaction between neighboring particles, which leads to slower approaching to saturation and hysteresis at high fields. However, the low field susceptibility is not influenced by the interaction, so that the particle size deduced from the low-field fit of Eq. (11) to the measured $M(H)$ curve is reliable, and in our modeling Eq. (1), the low-field $\chi_N(\omega)=\chi_{N0}$ is also justified.

The second partial superparamagnetism arises owing to the interaction between the nanoparticles within each nanosphere. The assembly of nanospheres is dilute in this case with magnetic nanospheres suspended in water undergoing Brownian motions. However, each sphere is not single domain but consisting of many single-domain particles, so that its dc magnetization can be precisely expressed by Eq. (11) only at low fields. For studying the properties of the nanospheres the classical superparamagnetic properties are extended to including the frequency dependence of low-field ac susceptibility, whose measuring time is comparable with the Brownian relaxation time.

Although both assemblies are partially superparamagnetic when the classical definition of superparamagnetism is concerned, they can be simply regarded as superparamagnetic if only low-field properties are considered, like our case of ac susceptibility measurements. In this case, both χ_N and χ_B are constants, which are calculated from Eq. (11) or Eq. (3) and originated from the field driven orientation of thermally agitated moments \mathbf{m}_0 that are much larger than atomic moments. It is interesting to see that although the M_0 for the second case is much smaller than for the first case, low-frequency χ'_B is comparable to χ'_N . The reason is that m_0 per sphere in the second case is 17 times m_0 per particle in the first case, so that the field driven moment rotation is 17 times enhanced by the increase in Zeeman energy.

The appearance of a finite residual m_0 for the spheres may be attributed to structural and thermal fluctuations, so that this m_0 should be understood as an average value in the second case. It is interesting to study how such fluctuations can lead to a basically sphere-size independent average m_0 , so that the value of m_0 becomes controllable for different kind of applications.

V. CONCLUSION

In conclusion, we have measured $\chi(f)$ of colloids containing magnetic nanospheres, each sphere consisting of many Fe_3O_4 nanoparticles uniformly embedded in a polystyrene matrix. Based on Debye's theory for $\chi(f)$ of magnetic

colloids where nanospheres undergo rotational Brownian motion, the measured results are consistent with the hydrodynamic size distribution $p(D)$ derived from translational Brownian motion detected by dynamic light scattering, as far as the moment of each nanosphere is assumed to be identical. Therefore, the magnetic moment carried by each nanosphere is demonstrated to be size independent. Since each sphere is an aggregation of single-domain particles mutually interacting antiferromagnetically, this moment should be an averaged small residual moment owing to structural and thermal fluctuations, of which detailed mechanism is to be elucidated in the future.

ACKNOWLEDGMENTS

Financial support from Consolider Project No. CSD2007-00041 and Catalan Project Nos. 2005SGR00731 and XaRMAE is acknowledged.

- ¹H. Xu, L.-L. Cui, N.-H. Tong, and H.-C. Gu, *J. Am. Chem. Soc.* **128**, 15582 (2006).
- ²J. Connolly and T. G. St Pierre, *J. Magn. Magn. Mater.* **225**, 156 (2001).
- ³J. Nutting, J. Antony, D. Meyer, A. Sharma, and Y. Qiang, *J. Appl. Phys.* **99**, 08B319 (2006).
- ⁴F. O. Ayorinde, S. V. Gelain, J. H. Johnson, Jr., and L. W. Wan, *Rapid Commun. Mass Spectrom.* **14**, 2116 (2000).
- ⁵D.-X. Chen, *Meas. Sci. Technol.* **15**, 1195 (2004).
- ⁶D.-X. Chen and C. Gu, *IEEE Trans. Magn.* **41**, 2436 (2005).
- ⁷R. Kötz, W. Weitschies, L. Trahms, W. Brewer, and W. Semmler, *J. Magn. Magn. Mater.* **194**, 62 (1999).
- ⁸P. C. Fannin, S. W. Charles, P. Kocpansky, M. Timko, V. Ocelik, M. Koneracka, L. Tomco, I. Turek, J. Stelina, and C. Musil, *Czech. J. Phys.* **51**, 599 (2001).
- ⁹S. H. Chung, A. Hoffmann, S. D. Bader, C. Liu, B. Kay, L. Makowski, and L. Chen, *Appl. Phys. Lett.* **85**, 2971 (2004).
- ¹⁰C.-Y. Hong, C. C. Wu, Y. C. Chiu, S. Y. Yang, H. E. Horng, and H. C. Yang, *Appl. Phys. Lett.* **88**, 212512 (2006).
- ¹¹E. M. Claesson, B. H. Ern , and A. P. Philipse, *J. Phys.: Condens. Matter* **19**, 286102 (2007).
- ¹²P. Debye, *Polar Molecules* (Dover, New York, 1929), p. 77.
- ¹³S. Chikazumi, *Physics of Magnetism* (Wiley, New York, 1964), pp. 62 and 100.
- ¹⁴*CRC Handbook of Chemistry and Physics*, 87th ed. (Taylor & Francis, London, 2006).
- ¹⁵B. Fischer, B. Huke, M. L ck, and R. Hempelmann, *J. Magn. Magn. Mater.* **289**, 74 (2005).
- ¹⁶E. M. Claesson and A. P. Philipse, *Langmuir* **21**, 9412 (2005).
- ¹⁷C. P. Bean, *J. Appl. Phys.* **26**, 1381 (1955).
- ¹⁸C. P. Bean and J. D. Livingston, *J. Appl. Phys.* **30**, S120 (1959).
- ¹⁹L. N el, *Ann. Geophys.* **5**, 99 (1949).
- ²⁰B. H. Erne, M. Claesson, S. Sacanna, M. Klokkenburg, E. Bakelaar, and B. W. M. Kuipers, *J. Magn. Magn. Mater.* **311**, 145 (2007).
- ²¹L. N el, *C. R. Acad. Sci. URSS* **252**, 4075 (1961); English translation in *Selected Works of Louis N el*, edited by N. Kurti (Gordon and Breach, New York, 1988), p. 107.